

Low-dose  $^{123}\text{I}$ -metaiodobenzylguanidine diagnostic scan is inferior to  $^{131}\text{I}$ -metaiodobenzylguanidine posttreatment scan in detection of malignant pheochromocytoma and paraganglioma

メタデータ	言語: eng
	出版者:
	公開日: 2017-10-05
	キーワード (Ja):
	キーワード (En):
	作成者:
	メールアドレス:
URL	所属:
	<a href="http://hdl.handle.net/2297/29298">http://hdl.handle.net/2297/29298</a>

Low dose  $^{123}\text{I}$ -MIBG diagnostic scan is inferior to  $^{131}\text{I}$ -MIBG post-treatment scan in detection of malignant pheochromocytoma and paraganglioma

The short title of the article:  $^{123}\text{I}$ -MIBG scan and  $^{131}\text{I}$ -MIBG post-treatment scan

Daiki Kayano, Junichi Taki, Makoto Fukuoka, Hiroshi Wakabayashi, Anri Inaki, Ayane Nakamura, Seigo Kinuya

Daiki Kayano, Junichi Taki, Makoto Fukuoka, Hiroshi Wakabayashi, Anri Inaki, Ayane Nakamura, Seigo Kinuya: Department of Nuclear Medicine, Kanazawa University Hospital, 13-1 Takara-machi, Kanazawa, Ishikawa, 920-8641, Japan

The name and address of the author responsible for correspondence concerning the manuscript and the name and address of the author to whom requests for reprints: Daiki Kayano, Department of Nuclear Medicine, Kanazawa University Hospital, 13-1 Takara-machi, Kanazawa, Ishikawa, 920-8641, Japan

Telephone number: +81-76-265-2333

Facsimile number: +81-76-234-4257

e-mail: [kayano@nmd.m.kanazawa-u.ac.jp](mailto:kayano@nmd.m.kanazawa-u.ac.jp)

This research did not receive any support in the form of grants, equipment, drugs, or combination of these.

This research did not receive any funding from any of the following organizations: National Institutes of Health; Wellcome Trust; Howard Hughes Medical Institute; and others.

## Abstract

**Objective:** We assessed the lesion detectability of low dose diagnostic  $^{123}\text{I}$ -metaiodobenzylguanidine (MIBG) whole body scans obtained at 6 and 24 hours compared with post-treatment  $^{131}\text{I}$ -MIBG whole body scans in malignant pheochromocytoma and paraganglioma.

**Methods:** Scintigrams obtained in 15 patients with malignant pheochromocytoma and paraganglioma were retrospectively analyzed. Diagnostic scans were performed with 111MBq of  $^{123}\text{I}$ -MIBG. Therapeutic doses of  $^{131}\text{I}$ -MIBG (5.55 to 7.40GBq) were administrated and whole body scans were obtained at 2 to 5 days after  $^{131}\text{I}$ -MIBG administrations. We compared the number of lesions and the lesion-to-referent count ratios at 6 hours and 24 hours of  $^{123}\text{I}$ -MIBG and at 2 to 5 days of  $^{131}\text{I}$ -MIBG.

**Results:** In comparison with the 6-hour images of  $^{123}\text{I}$ -MIBG, the 24-hour images of  $^{123}\text{I}$ -MIBG could detect more lesions in 8 patients. Post-treatment  $^{131}\text{I}$ -MIBG scans revealed new lesions in 8 patients compared with the 24-hour images of  $^{123}\text{I}$ -MIBG. The lesion-to-referent count ratios at 6 hours and 24 hours of  $^{123}\text{I}$ -MIBG and at 3 days of  $^{131}\text{I}$ -MIBG were increasing at later scanning time. There were significant differences in the lesion-to-referent count ratios between 6 hours and 24 hours of  $^{123}\text{I}$ -MIBG ( $p = 0.031$ ), 6 hours of  $^{123}\text{I}$ -MIBG and 3 days of  $^{131}\text{I}$ -MIBG ( $p = 0.020$ ), and 24 hours of  $^{123}\text{I}$ -MIBG and 3 days of  $^{131}\text{I}$ -MIBG ( $p = 0.018$ ).

**Conclusions:** Low dose diagnostic  $^{123}\text{I}$ -MIBG whole body scan is inferior to post-treatment  $^{131}\text{I}$ -MIBG whole body scan in malignant pheochromocytoma and paraganglioma. Considering the scan timing of  $^{123}\text{I}$ -MIBG, 6-hour images might have no superiority compared with 24-hour images.

**Keywords:** pheochromocytoma; paraganglioma; MIBG;  $^{123}\text{I}$ ;  $^{131}\text{I}$ .

## Introduction

Metaiodobenzylguanidine (MIBG), which can be labeled with either  $^{131}\text{I}$  or  $^{123}\text{I}$ , mimics the neurotransmitter norepinephrine and specifically targets malignant cells of the sympathetic nervous system [1, 2]. Since  $^{131}\text{I}$ -MIBG was reported to visualize tumors of the adrenal medulla in the early 1980s [3, 4],  $^{131}\text{I}$ -MIBG and  $^{123}\text{I}$ -MIBG have been widely used for detecting lesions in patients with malignant neuroendocrine tumors, such as malignant pheochromocytomas, malignant paragangliomas, medullary thyroid carcinomas, carcinoid tumors and neuroblastomas [5-9].  $^{123}\text{I}$ -MIBG has superiority over  $^{131}\text{I}$ -MIBG with diagnostic use, because the  $\gamma$ -ray energy of  $^{123}\text{I}$  (159keV) befits the image quality and lesion detectability for scintigraphy compared with that of  $^{131}\text{I}$  (364keV) [10-12]. Moreover,  $^{123}\text{I}$  offers favorable dosimetry compared to  $^{131}\text{I}$ , because of their  $\gamma$ -ray energy and their half-life ( $^{123}\text{I}$ : 13.13 hours,  $^{131}\text{I}$ : 8.04 days) [13].

It has been reported that other imaging modalities may be useful in detecting neuroendocrine tumors. Many articles compared  $^{123}\text{I}$ -MIBG with  $^{18}\text{F}$ -fluoro-2-deoxy-D-glucose ( $^{18}\text{F}$ -FDG) positron emission tomography (PET) or  $^{18}\text{F}$ -FDG PET/computed tomography (CT) have been reported. These articles did not show good concordance [14-17], therefore  $^{123}\text{I}$ -MIBG and  $^{18}\text{F}$ -FDG PET would possess complementary roles.  $^{18}\text{F}$ -3,4-dihydroxy-phenylalanine PET,  $^{18}\text{F}$ -fluorodopamine PET and  $^{68}\text{Ga}$ -DOTA peptides PET might be preferred in comparison with  $^{123}\text{I}$ -MIBG [17, 18]. However, the evidence for these radiopharmaceuticals is insufficient and these have not become widely used yet.

As a prelude to  $^{131}\text{I}$ -MIBG therapy,  $^{123}\text{I}$ -MIBG scintigraphy is essential for the confirmation of MIBG accumulation to lesions. After  $^{131}\text{I}$ -MIBG therapy, post-treatment  $^{131}\text{I}$ -MIBG scintigraphy is routinely used to assess tumor uptake rather than lesion detectability. Lesional detectability of  $^{123}\text{I}$ -MIBG scans was not always the same as that of post-treatment  $^{131}\text{I}$ -MIBG scans. Campbell et al. [19] reported a case in which the post-treatment  $^{131}\text{I}$ -MIBG image depicted more metastatic lesions compared with the  $^{131}\text{I}$ -MIBG diagnostic scan and  $^{123}\text{I}$ -MIBG scan in a patient with malignant pheochromocytoma. Fukuoka et al. [20] demonstrated that 3-day images of post-therapeutic  $^{131}\text{I}$ -MIBG had superiority over 6-hour images of low dose

diagnostic  $^{123}\text{I}$ -MIBG in patients with malignant pheochromocytomas, malignant paragangliomas and neuroblastomas. Considering the lesion-to-background count ratios of  $^{123}\text{I}$ -MIBG images, 6-hour images would be inferior to 24-hour images in detecting lesions. To our knowledge, most previous studies evaluated scintigrams only by visual assessment, and there is no literature that reports the quantitative analysis of the image based on the count density and the lesion detectability between 6 and 24-hour scans of diagnostic  $^{123}\text{I}$ -MIBG and post-therapeutic  $^{131}\text{I}$ -MIBG scans.

In this study, we compared low dose diagnostic  $^{123}\text{I}$ -MIBG scans obtained at 6 hours, at 24 hours, and post-treatment  $^{131}\text{I}$ -MIBG scans by visual and quantitative methods in detecting lesions of malignant pheochromocytoma and paraganglioma, and then evaluated the validity of the dose and the scanning time of  $^{123}\text{I}$ -MIBG scintigraphy.

## **Methods**

### **Patients**

We studied 15 consecutive patients who underwent first  $^{131}\text{I}$ -MIBG therapy for adult malignant pheochromocytoma and paraganglioma between March 2005 and March 2010. The patients comprised 9 males and 6 females, and the age range was 37 to 78 years (mean = 57.1 years). Twelve were malignant pheochromocytomas and three were malignant paragangliomas (Table 1). In all patients, we confirmed MIBG accumulations in the primary or metastatic lesions with diagnostic  $^{123}\text{I}$ -MIBG scintigraphy before  $^{131}\text{I}$ -MIBG therapy.

### **Low dose diagnostic $^{123}\text{I}$ -MIBG scintigraphy**

We performed  $^{123}\text{I}$ -MIBG scintigraphy after intravenous injection of 111MBq of  $^{123}\text{I}$ -MIBG (FUJIFILM RI Pharma Co., Ltd., Japan), using a dual-head gamma camera equipped with a low-medium energy general purpose collimator (Toshiba E-CAM, Japan or Siemens Medical Solutions Symbia, Germany), specifically designed for reduced the scatter and septal penetration of the small fraction of  $^{123}\text{I}$  high-energy photons. The activity of  $^{123}\text{I}$ -MIBG was assayed by the supplier to become 111MBq at noon of the administration day. In this study, the dose of  $^{123}\text{I}$ -MIBG was relatively low compared to the standard dose of  $^{123}\text{I}$ -MIBG in Western countries, which was approved up to 400MBq [13, 21], because only 111MBq of  $^{123}\text{I}$ -MIBG had

been available for adults due to Japanese regulations until October 2010. Whole body scans were obtained at 6 and 24 hours after  $^{123}\text{I}$ -MIBG administration with 15cm/min of scanning speed on a photo peak of 159keV with a 15% window.

### **$^{131}\text{I}$ -MIBG therapy and post-therapeutic scintigraphy**

$^{131}\text{I}$ -MIBG therapy was performed 2 to 21 days (mean = 11.9 days) after diagnostic  $^{123}\text{I}$ -MIBG scintigraphy. To prevent thyroidal uptake of free iodine, oral administration of 200mg potassium iodide was commenced one day before  $^{131}\text{I}$ -MIBG administration and continued for up to 10 days post therapy. We intravenously administrated 5.55 to 7.4GBq (mean = 7.28GBq) of  $^{131}\text{I}$ -MIBG through fixed peripheral venous lines for about an hour using a lead-shielded infusion pump with monitoring vital signs for more than 6 hours from the beginning of  $^{131}\text{I}$ -MIBG administration. All patients were treated in the isolation room until radiation decreased to less than 30 $\mu\text{Sv/hr}$  at 1m. All therapies were well tolerated. A whole body scan with therapeutic dose of  $^{131}\text{I}$ -MIBG was obtained once at 2 to 5 days (mean = 3.4 days) after injection with 15cm/min of scanning speed on a photo peak of 364keV with a 15% window, using a high energy collimator. Table 1 shows the dosage and the scanning time of  $^{131}\text{I}$ -MIBG therapy.

### **Visual evaluation**

Two experienced nuclear medicine physicians of our institution, who were blinded to the findings of the other imaging modalities, evaluated the accumulations of 6 and 24-hour images of  $^{123}\text{I}$ -MIBG and a post-treatment  $^{131}\text{I}$ -MIBG image. They interpreted all foci except for physiological accumulation as abnormal uptake and defined their anatomical location. Diffuse accumulation at nasal cavity, salivary glands, thyroid, myocardium, liver and bladder were considered as physiological uptake. When small lesions or low MIBG uptake lesions are overlapped with physiological (e.g. liver) uptake, some lesions might be undetected. When their interpretation was discordant, they obtained consensus after conference. To compare the lesion detectability of 6 and 24-hour images of  $^{123}\text{I}$ -MIBG with a post-treatment  $^{131}\text{I}$ -MIBG image, we investigated the difference in the number of detected lesions in the following 4 sites: bone, lungs, liver and others.

### Quantitative evaluation

As a quantitative evaluation, we used the uptake ratio. On anterior and posterior images at 24 hours of  $^{123}\text{I}$ -MIBG, a target region of interest (ROI) was set manually by tracing the margin of the most intense lesion and a referential ROI and a background (BG) ROI were set on the left thigh and the background. The same ROIs were used on each image at 6 hours of  $^{123}\text{I}$ -MIBG and at 3 days of  $^{131}\text{I}$ -MIBG. In cases where metastatic lesions existed in the left thigh, the right thigh was used as a referential ROI. The uptake ratio was calculated with each mean ROI count by the following formula: uptake ratio = (target ROI – BG ROI) / (referential ROI – BG ROI). We compared the uptake ratios at 6 hours and 24 hours of  $^{123}\text{I}$ -MIBG and at 3 days of  $^{131}\text{I}$ -MIBG. To standardize the scanning time, we evaluated 10 patients whose  $^{131}\text{I}$ -MIBG scans were obtained at 3 days after  $^{131}\text{I}$ -MIBG therapies.

### Statistical analysis

The paired t-test was used for analysis of the sequential changes of the uptake ratios between 6 hours and 24 hours after  $^{123}\text{I}$ -MIBG injections and 3 days after  $^{131}\text{I}$ -MIBG administrations. A p value of less than 0.05 was considered as the significant difference.

### Results

A total of 96 and 106 lesions were identified with 6 and 24-hour images of  $^{123}\text{I}$ -MIBG, respectively.  $^{131}\text{I}$ -MIBG post-treatment scans detected 170 lesions. Table 2 summarizes visual analyses. In comparison to the 6-hour images of  $^{123}\text{I}$ -MIBG, the 24-hour images of  $^{123}\text{I}$ -MIBG could detect more lesions in 8 (53%) of 15 patients. In all patients, the 6-hour images of  $^{123}\text{I}$ -MIBG had no advantage compared with the 24-hour images of  $^{123}\text{I}$ -MIBG in detecting lesions. In comparison between diagnostic  $^{123}\text{I}$ -MIBG scans and post-treatment  $^{131}\text{I}$ -MIBG scans, post-treatment  $^{131}\text{I}$ -MIBG scans had better lesional detectability than diagnostic  $^{123}\text{I}$ -MIBG scans in 8 (53%) of 15 patients.  $^{123}\text{I}$ -MIBG scans were not superior to  $^{131}\text{I}$ -MIBG scans in any cases. Table 3 shows the number of detected lesions in bone, lungs, liver and others with diagnostic  $^{123}\text{I}$ -MIBG scans and post-therapeutic  $^{131}\text{I}$ -MIBG scans.  $^{123}\text{I}$ -MIBG scans could detect lesions in 56% (64/115) of bone metastases, 64%

(9/14) of lung metastases, 88% (15/17) of liver metastases, 75% (18/24) of metastases in others, and 62% (106/170) of all lesions compared with post-therapeutic  $^{131}\text{I}$ -MIBG scans.

Fig. 1 shows time-course changes of uptake ratios in 10 patients whose  $^{131}\text{I}$ -MIBG scans were obtained at 3 days after  $^{131}\text{I}$ -MIBG therapies. The uptake ratios were higher at later scanning time. There were significant differences in the uptake ratios between 6 hours and 24 hours of  $^{123}\text{I}$ -MIBG ( $p = 0.031$ ), 6 hours of  $^{123}\text{I}$ -MIBG and 3 days of  $^{131}\text{I}$ -MIBG ( $p = 0.020$ ), and 24 hours of  $^{123}\text{I}$ -MIBG and 3 days of  $^{131}\text{I}$ -MIBG ( $p = 0.018$ ).

Fig. 2 and Fig. 3 show the representative scans of  $^{123}\text{I}$ -MIBG and  $^{131}\text{I}$ -MIBG. In Figure 2, the 24-hour image of  $^{123}\text{I}$ -MIBG excelled in the lesion detectability compared with the 6-hour image of  $^{123}\text{I}$ -MIBG. The number of lesions between  $^{123}\text{I}$ -MIBG and  $^{131}\text{I}$ -MIBG was the same. However, the lesion was better visualized in the  $^{131}\text{I}$ -MIBG image than in the  $^{123}\text{I}$ -MIBG image, which was confirmed by the quantitative analysis using uptake ratios. Figure 3 shows that  $^{131}\text{I}$ -MIBG was superior to  $^{123}\text{I}$ -MIBG in both visual and quantitative assessment.

## Discussion

In this study, we demonstrated with visual and quantitative methods that low dose  $^{123}\text{I}$ -MIBG (111MBq) scans were not suitable for detecting lesions compared with post-treatment  $^{131}\text{I}$ -MIBG scans.

Our results were likely due to at least two reasons. Firstly, the diagnostic dose of  $^{123}\text{I}$ -MIBG was significantly lower compared with the therapeutic dose of  $^{131}\text{I}$ -MIBG. In the report by Ali et al. [22], the combination of the modern gamma camera with a low energy collimator and  $^{123}\text{I}$  imaging showed a count rate of up to 20-fold greater compared with an equivalent activity of  $^{131}\text{I}$ , because of the characteristics of  $^{123}\text{I}$  and  $^{131}\text{I}$ . Therefore, a dose of 185MBq  $^{123}\text{I}$  was equivalent to almost 3.7GBq  $^{131}\text{I}$  in image quality in patients with thyroid cancer. Iwano et al. [23] reported that the diagnostic scan with 37MBq of  $^{123}\text{I}$  was not always predictive of subsequent therapeutic  $^{131}\text{I}$  uptake in detecting residual thyroid tissue and metastases of differentiated thyroid cancer. Donahue et al. [24] concluded that



post-treatment  $^{131}\text{I}$  whole body scans provided incremental clinically relevant information in addition to pre-treatment  $^{123}\text{I}$  whole body scans in 10% of patients with differentiated thyroid cancer. Considering the same pharmaceutical kinetics of  $^{123}\text{I}$ -MIBG and  $^{131}\text{I}$ -MIBG, a diagnostic dose of  $^{123}\text{I}$ -MIBG was assumed to be equal in imaging quality to a 20-fold greater  $^{131}\text{I}$ -MIBG dose. In our study, the doses of  $^{123}\text{I}$ -MIBG (111MBq) were less than one-fiftieth of the doses of  $^{131}\text{I}$ -MIBG (5.55 to 7.4GBq). To improve the lesion detectability with  $^{123}\text{I}$ -MIBG, the dose of  $^{123}\text{I}$ -MIBG should be increased. Considering that the standard doses of  $^{131}\text{I}$ -MIBG therapy for malignant pheochromocytoma and paraganglioma are more than 7.4GBq [25-27], more than 370MBq of  $^{123}\text{I}$ -MIBG might be desirable to detect lesions of malignant pheochromocytoma and paraganglioma.

Another likely reason for our results was the difference of scanning time after MIBG injections between  $^{123}\text{I}$ -MIBG and  $^{131}\text{I}$ -MIBG. In this study, the 24-hour images of  $^{123}\text{I}$ -MIBG could detect more lesions than the 6-hour images of  $^{123}\text{I}$ -MIBG in 8 (53%) of 15 patients. Furthermore, the 2 to 5-day images of  $^{131}\text{I}$ -MIBG were superior to the 24-hour images of  $^{123}\text{I}$ -MIBG in 8 (53%) of 15 patients. As shown in Figure 1, we demonstrated that the lesion-to-referent count ratios increased at later scanning time. These results indicated that early scan timing after  $^{123}\text{I}$ -MIBG injection was not recommended. The European Association of Nuclear Medicine guidelines suggest that scanning with  $^{123}\text{I}$ -MIBG is performed between 20 and 24 hours after injection and selected delayed images (never later than day 2) might be useful in the event of equivocal findings on day 1 [13, 28]. In contrast, the Japanese Ministry of Health, Labor and Welfare established that  $^{123}\text{I}$ -MIBG scanning was performed at 24 hours after injection and additional images might be obtained at 6 or 48 hours after administration if needed. Our results indicated that 6-hour images after  $^{123}\text{I}$ -MIBG injection would not be necessary. Even if small lesions or low uptake lesions are located in or near the kidneys and excretory route that may be masked by uptake in these areas, 6-hour images may not aid the visualization of lesions because physiological uptake of MIBG is more intense in early image than late image.

Diagnostic scintigraphy with low dose  $^{123}\text{I}$ -MIBG has limitations in detecting lesions of malignant pheochromocytoma and malignant paraganglioma. The

possible discrepancy between low dose diagnostic  $^{123}\text{I}$ -MIBG and post-treatment  $^{131}\text{I}$ -MIBG scans should be taken into account when developing a treatment plan. An  $^{131}\text{I}$ -MIBG post-treatment scan might provide us with more clinical information in patients with malignant pheochromocytoma and malignant paraganglioma. We recommended that patients who had small lesions that were not detected with a low dose  $^{123}\text{I}$ -MIBG scan but confirmed with other imaging modalities, such as CT and magnetic resonance imaging, be considered for  $^{131}\text{I}$ -MIBG therapy if their primary lesion that had been surgically excised had accumulated MIBG.

Our study had some limitations. One limitation was that the dose of  $^{123}\text{I}$ -MIBG of our study was lower than that of the standard dose of  $^{123}\text{I}$ -MIBG in Western countries. Another limitation was that the scanning speed of  $^{123}\text{I}$ -MIBG scintigraphy was higher than that recommended by EANM guidelines (15cm/min compared to the guidance of 5cm/min) [13]. The low dose and the fast scanning speed of  $^{123}\text{I}$ -MIBG would decrease signal-to-noise ratio compared with the high dose and the slow scanning speed. Those would result in the reduction of not only the lesional detectability of visual evaluation but the uptake ratio of quantitative evaluation of  $^{123}\text{I}$ -MIBG scintigraphy. In this study, we did not evaluate the detectability of single photon emission computed tomography (SPECT)/CT. SPECT/CT is now getting popular as a daily practice. This would certainly enhance the detection of the lesion with in the areas of physiological uptake (e.g. liver) and the lesion that overlapped on the physiological uptake (e.g. bladder) on planar whole-body imaging.

In conclusion, a low dose diagnostic  $^{123}\text{I}$ -MIBG scan has limitations compared to post-treatment  $^{131}\text{I}$ -MIBG scan. Compared with a 24-hour image of  $^{123}\text{I}$ -MIBG, a 6-hour image of  $^{123}\text{I}$ -MIBG has no advantage in detecting lesions of malignant pheochromocytoma and malignant paraganglioma. The escalation of  $^{123}\text{I}$ -MIBG doses might be beneficial for the diagnosis of distribution of metastasis.

## References

- 1 Jaques S, Jr., Tobes MC, Sisson JC. Sodium dependency of uptake of norepinephrine and m-iodobenzylguanidine into cultured human pheochromocytoma cells: evidence for uptake-one. *Cancer Res* 1987; **47**:3920-3928.
- 2 Ilias I, Pacak K. Current approaches and recommended algorithm for the diagnostic localization of pheochromocytoma. *J Clin Endocrinol Metab* 2004; **89**:479-491.
- 3 Wieland DM, Wu J, Brown LE, Mangner TJ, Swanson DP, Beierwaltes WH. Radiolabeled adrenergi neuron-blocking agents: adrenomedullary imaging with [131I]iodobenzylguanidine. *J Nucl Med* 1980; **21**:349-353.
- 4 Nakajo M, Shapiro B, Copp J, Kalff V, Gross MD, Sisson JC et al. The normal and abnormal distribution of the adrenomedullary imaging agent m-[I-131]iodobenzylguanidine (I-131 MIBG) in man: evaluation by scintigraphy. *J Nucl Med* 1983; **24**:672-682.
- 5 Sisson JC, Frager MS, Valk TW, Gross MD, Swanson DP, Wieland DM et al. Scintigraphic localization of pheochromocytoma. *N Engl J Med* 1981; **305**:12-17.
- 6 Shapiro B, Copp JE, Sisson JC, Eyre PL, Wallis J, Beierwaltes WH. Iodine-131 metaiodobenzylguanidine for the locating of suspected pheochromocytoma: experience in 400 cases. *J Nucl Med* 1985; **26**:576-585.
- 7 Sisson JC, Shulkin BL. Nuclear medicine imaging of pheochromocytoma and neuroblastoma. *Q J Nucl Med* 1999; **43**:217-223.
- 8 Rufini V, Castaldi P, Treglia G, Perotti G, Gross MD, Al-Nahhas A et al. Nuclear medicine procedures in the diagnosis and therapy of medullary thyroid carcinoma. *Biomed Pharmacother* 2008; **62**:139-146.
- 9 Jacobson AF, Deng H, Lombard J, Lessig HJ, Black RR. 123I-meta-iodobenzylguanidine scintigraphy for the detection of neuroblastoma and pheochromocytoma: results of a meta-analysis. *J Clin Endocrinol Metab* 2010; **95**:2596-2606.
- 10 Furuta N, Kiyota H, Yoshigoe F, Hasegawa N, Ohishi Y. Diagnosis of pheochromocytoma using [123I]-compared with [131I]-metaiodobenzylguanidine scintigraphy. *Int J Urol* 1999; **6**:119-124.
- 11 Koopmans KP, Neels ON, Kema IP, Elsinga PH, Links TP, de Vries EG et al. Molecular imaging in neuroendocrine tumors: molecular uptake

mechanisms and clinical results. *Crit Rev Oncol Hematol* 2009; **71**:199-213.

12 Adler JT, Meyer-Rochow GY, Chen H, Benn DE, Robinson BG, Sippel RS et al. Pheochromocytoma: current approaches and future directions. *Oncologist* 2008; **13**:779-793.

13 Bombardieri E, Giammarile F, Aktolun C, Baum RP, Bischof Delaloye A, Maffioli L et al. <sup>131</sup>I/<sup>123</sup>I-metaiodobenzylguanidine (mIBG) scintigraphy: procedure guidelines for tumour imaging. *Eur J Nucl Med Mol Imaging* 2010; **37**:2436-2446.

14 Taggart DR, Han MM, Quach A, Groshen S, Ye W, Villablanca JG et al. Comparison of iodine-123 metaiodobenzylguanidine (MIBG) scan and [<sup>18</sup>F]fluorodeoxyglucose positron emission tomography to evaluate response after iodine-131 MIBG therapy for relapsed neuroblastoma. *J Clin Oncol* 2009; **27**:5343-5349.

15 Sharp SE, Shulkin BL, Gelfand MJ, Salisbury S, Furman WL. <sup>123</sup>I-MIBG scintigraphy and <sup>18</sup>F-FDG PET in neuroblastoma. *J Nucl Med* 2009; **50**:1237-1243.

16 Papathanasiou ND, Gaze MN, Sullivan K, Aldridge M, Waddington W, Almuhaideb A et al. <sup>18</sup>F-FDG PET/CT and <sup>123</sup>I-metaiodobenzylguanidine imaging in high-risk neuroblastoma: diagnostic comparison and survival analysis. *J Nucl Med* 2011; **52**:519-525.

17 Timmers HJ, Chen CC, Carrasquillo JA, Whatley M, Ling A, Havekes B et al. Comparison of <sup>18</sup>F-fluoro-L-DOPA, <sup>18</sup>F-fluoro-deoxyglucose, and <sup>18</sup>F-fluorodopamine PET and <sup>123</sup>I-MIBG scintigraphy in the localization of pheochromocytoma and paraganglioma. *J Clin Endocrinol Metab* 2009; **94**:4757-4767.

18 Kroiss A, Putzer D, Uprimny C, Decristoforo C, Gabriel M, Santner W et al. Functional imaging in phaeochromocytoma and neuroblastoma with <sup>68</sup>Ga-DOTA-Tyr <sup>3</sup>-octreotide positron emission tomography and <sup>123</sup>I-metaiodobenzylguanidine. *Eur J Nucl Med Mol Imaging* 2011; **38**:865-873.

19 Campbell L, Mouratidis B, Sullivan P. Improved detection of disseminated pheochromocytoma using post therapy I-131 MIBG scanning. *Clin Nucl Med* 1996; **21**:960-963.

20 Fukuoka M, Taki J, Mochizuki T, Kinuya S. Comparison of diagnostic value of I-123 MIBG and high-dose I-131 MIBG scintigraphy including incremental value of SPECT/CT over planar image in patients with

malignant pheochromocytoma/paraganglioma and neuroblastoma. Clin Nucl Med 2011; **36**:1-7.

21 Rufini V, Calcagni ML, Baum RP. Imaging of neuroendocrine tumors. Semin Nucl Med 2006; **36**:228-247.

22 Ali N, Sebastian C, Foley RR, Murray I, Canizales AL, Jenkins PJ et al. The management of differentiated thyroid cancer using 123I for imaging to assess the need for 131I therapy. Nucl Med Commun 2006; **27**:165-169.

23 Iwano S, Kato K, Nihashi T, Ito S, Tachi Y, Naganawa S. Comparisons of I-123 diagnostic and I-131 post-treatment scans for detecting residual thyroid tissue and metastases of differentiated thyroid cancer. Ann Nucl Med 2009; **23**:777-782.

24 Donahue KP, Shah NP, Lee SL, Oates ME. Initial staging of differentiated thyroid carcinoma: continued utility of posttherapy 131I whole-body scintigraphy. Radiology 2008; **246**:887-894.

25 Gedik GK, Hoefnagel CA, Bais E, Olmos RA. 131I-MIBG therapy in metastatic pheochromocytoma and paraganglioma. Eur J Nucl Med Mol Imaging 2008; **35**:725-733.

26 Safford SD, Coleman RE, Gockerman JP, Moore J, Feldman JM, Leight GS, Jr. et al. Iodine -131 metaiodobenzylguanidine is an effective treatment for malignant pheochromocytoma and paraganglioma. Surgery 2003; **134**:956-962; discussion 962-963.

27 Fitzgerald PA, Goldsby RE, Huberty JP, Price DC, Hawkins RA, Veatch JJ et al. Malignant pheochromocytomas and paragangliomas: a phase II study of therapy with high-dose 131I-metaiodobenzylguanidine (131I-MIBG). Ann N Y Acad Sci 2006; **1073**:465-490.

28 Olivier P, Colarinha P, Fettich J, Fischer S, Frokier J, Giammarile F et al. Guidelines for radioiodinated MIBG scintigraphy in children. Eur J Nucl Med Mol Imaging 2003; **30**:B45-50.

**Legends for illustrations**

Fig. 1 Time-course changes of uptake ratios. The uptake ratios are higher at later scanning time. Because no abnormal accumulation is detected on the 6-hour image of  $^{123}\text{I}$ -MIBG in patient number 12 in table 1 and table 2, the paired t-tests are performed among 9 patients between 6 hours and 24 hours of  $^{123}\text{I}$ -MIBG and between 6 hours of  $^{123}\text{I}$ -MIBG and 3 days of  $^{131}\text{I}$ -MIBG and among 10 patients between 24 hours of  $^{123}\text{I}$ -MIBG and 3 days of  $^{131}\text{I}$ -MIBG.

Fig. 2 A 37-year-old female with pheochromocytoma, patient number 12 in table 1 and table 2. No abnormal accumulation is seen on the 6-hour image of  $^{123}\text{I}$ -MIBG. The 24-hour image of  $^{123}\text{I}$ -MIBG can identify a faint accumulation in the right mid abdomen and the 3-day image of  $^{131}\text{I}$ -MIBG can identify a strong accumulation in the same lesion (arrows). No additional uptake is detected on the 3-day image of  $^{131}\text{I}$ -MIBG. Uptake ratios of the right mid abdomen lesion are 3.55 and 5.80 on the 24-hour image of  $^{123}\text{I}$ -MIBG and the 3-day image of  $^{131}\text{I}$ -MIBG. The uptake ratio of the 6-hour image of  $^{123}\text{I}$ -MIBG cannot be calculated because no lesional uptake is detected on the 6-hour image of  $^{123}\text{I}$ -MIBG.

Fig. 3 A 78-year-old female with pheochromocytoma, patient number 3 in table 1 and table 2. A total of 7 lesions are detected in the bone with the 6 and 24-hour images of  $^{123}\text{I}$ -MIBG (narrow arrows on each anterior image of  $^{123}\text{I}$ -MIBG). Same lesions are detected (narrow arrows on the anterior image of  $^{131}\text{I}$ -MIBG) and 7 new lesions can be identified with the 3-day image of  $^{131}\text{I}$ -MIBG (wide arrows on the posterior image of  $^{131}\text{I}$ -MIBG). The uptake ratios of the lumbar spine (arrow heads on each anterior image of  $^{123}\text{I}$ -MIBG and  $^{131}\text{I}$ -MIBG) are 5.33, 9.21, and 27.07 on each image.



## Tables

Table 1 Clinical characteristics and protocol of  $^{131}\text{I}$ -MIBG therapy

Patient				$^{131}\text{I}$ -MIBG	
Number	Age	Sex	Diagnosis	Dose (GBq)	Scanning time (days)
1	43	M	pheo	7.4	5
2	46	M	para	7.4	5
3	78	F	pheo	7.4	3
4	76	M	pheo	7.4	4
5	52	M	pheo	7.4	5
6	63	M	pheo	7.4	3
7	45	M	pheo	7.4	3
8	75	M	pheo	5.55	2
9	61	M	para	7.4	3
10	69	M	pheo	7.4	3
11	60	F	pheo	7.4	3
12	37	F	pheo	7.4	3
13	54	F	para	7.4	3
14	39	F	pheo	7.4	3
15	58	F	pheo	7.4	3

MIBG, metaiodobenzylguanidine; pheo, malignant pheochromocytoma; para, malignant paraganglioma.

Table 2 The number of lesions on diagnostic  $^{123}\text{I}$ -MIBG scans (6 and 24 hours) and post-treatment  $^{131}\text{I}$ -MIBG scans (2 to 5 days)

Patient Number	$^{123}\text{I}$ -MIBG		$^{131}\text{I}$ -MIBG
	6 hours	24 hours	2 to 5 days
1	9	10	10
2	5	5	5
3	7	7	14
4	10	10	13
5	1	1	1
6	3	3	9
7	5	6	6
8	3	4	6
9	23	24	45
10	1	2	2
11	6	6	6
12	0	1	1
13	1	1	4
14	6	9	17
15	16	17	31
Total	96	106	170

MIBG, metaiodobenzylguanidine.

Table 3 The number of detected lesions in bone, lung, liver and others with diagnostic  $^{123}\text{I}$ -MIBG scans and post-treatment  $^{131}\text{I}$ -MIBG scans

	Bone	Lung	Liver	Others	Total
$^{123}\text{I}$ -MIBG scan (n)	64	9	15	18	106
$^{131}\text{I}$ -MIBG scan (n)	115	14	17	24	170

MIBG, metaiodobenzylguanidine.

Illustrations

Fig. 1

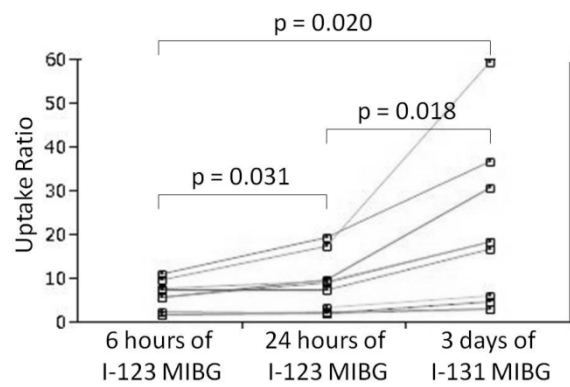


Fig. 2

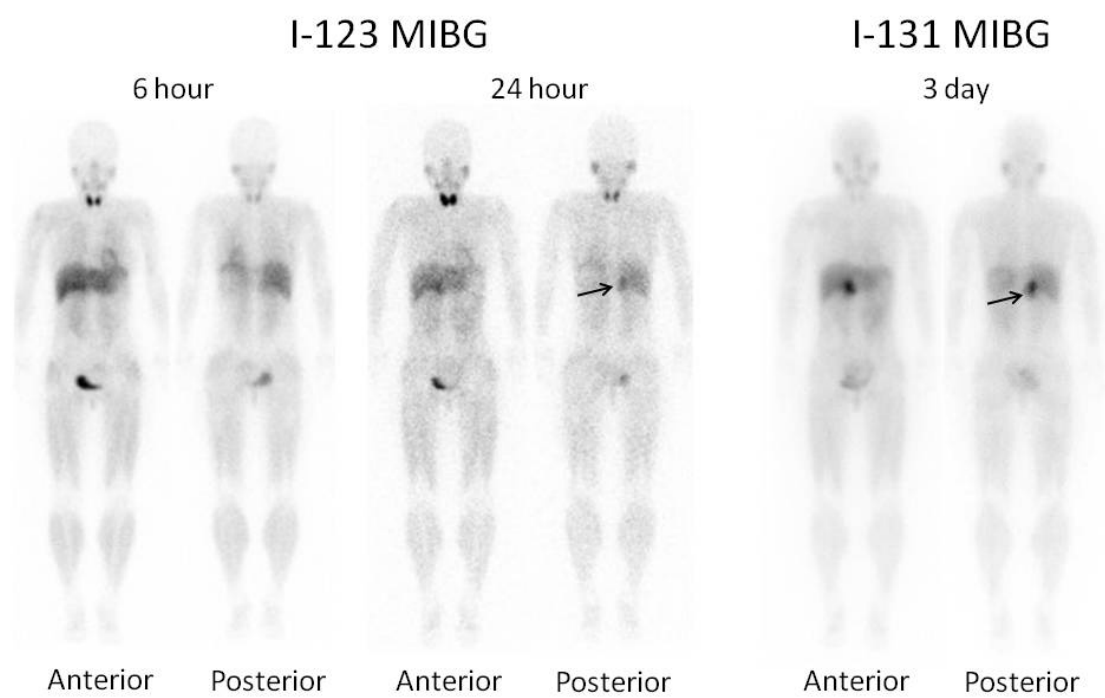


Fig. 3

